

# Entanglement distribution over quantum code-division-multiple-access networks

Chang-long Zhu,<sup>1,2</sup> Nan Yang,<sup>1,2</sup> Yu-xi Liu,<sup>3,2</sup> Franco Nori,<sup>4,5</sup> and Jing Zhang<sup>1,2,\*</sup>

<sup>1</sup>*Department of Automation, Tsinghua University, Beijing 100084, P. R. China*

<sup>2</sup>*Center for Quantum Information Science and Technology, TNList, Beijing 100084, P. R. China*

<sup>3</sup>*Institute of Microelectronics, Tsinghua University, Beijing 100084, P. R. China*

<sup>4</sup>*CEMS, RIKEN, Saitama 351-0198, Japan*

<sup>5</sup>*Physics Department, The University of Michigan, Ann Arbor, Michigan 48109-1040, USA*

(Dated: July 12, 2021)

We present a method for quantum entanglement distribution over a so-called code-division-multiple-access network, in which two pairs of users share the same quantum channel to transmit information. The main idea of this method is to use different broad-band chaotic phase shifts, generated by electro-optic modulators (EOMs) and chaotic Colpitts circuits, to encode the information-bearing quantum signals coming from different users, and then recover the masked quantum signals at the receiver side by imposing opposite chaotic phase shifts. The chaotic phase shifts given to different pairs of users are almost uncorrelated due to the randomness of chaos and thus the quantum signals from different pair of users can be distinguished even when they are sent via the same quantum channel. It is shown that two maximally-entangled states can be generated between two pairs of users by our method mediated by bright coherent lights, which can be more easily implemented in experiments compared with single-photon lights. Our method is robust under the channel noises if only the decay rates of the information-bearing fields induced by the channel noises are not quite high. Our study opens up new perspectives for addressing and transmitting quantum information in future quantum networks.

PACS numbers: 89.70.-a, 42.79.Sz, 62.25.Jk

## I. INTRODUCTION

With recent progresses in various quantum systems, such as ion-trap systems [1–3] and solid-state quantum circuits [4–6], it is now possible to discuss how to establish more efficient quantum networks or so-called quantum internet [7]. The existing studies about quantum communication [8–10] and quantum cryptography [11, 12] have shown that quantum network has great advantages to transfer classical or quantum information. However, how to best transfer information via quantum networks is still an open problem [13–23].

To transfer quantum information over a large-scale quantum network, a question is: can we allow different pairs of users, who want to transmit information, to share the same channel [24–26]. This problem has been widely discussed in the field of classical communication [27, 28]. In classical communication systems, such kind of methods are called channel-access methods or multiple-access methods. There are mainly four different kinds of multiple-access methods [29]: the frequency-division multiple access (FDMA) methods, the time-division multiple access (TDMA) methods, the code-division multiple access (CDMA) methods, and the orthogonal-frequency division multiple access (OFDMA) methods. In FDMA methods, different frequency bands are assigned to different data streams, while in TDMA methods the users split their signals into pieces and transmitted them at

different time slots to share the same channel. TDMA and FDMA work equally well and are the key techniques for the first generation (analog) and the second generation (digital) mobile networks. In CDMA methods, each pair of users shares the same channel and distinguishes with each other by their own unique codes. It can be shown that CDMA can accommodate more bits per channel use, compared with TDMA and FDMA [30], and thus is used in third-generation mobile communication systems. However, the interference between different data streams will deteriorate the information rate of CDMA. Other competitive approaches are proposed including orthogonal frequency-division multiple-access (OFDMA), in which the available subcarriers are divided into several mutually orthogonal subchannels which are assigned to distinct users for simultaneous transmission. The OFDMA is capable of avoiding the interference problem and thus provide better performance in classical *digital* communication.

Although the multiple-access problem has been widely studied in classical communication, it is considered in quantum communication only recently due to the development of techniques for scalable quantum network. To our knowledge, FDMA, or equivalently, the so-called wavelength-division multiple access (WDMA), has been used for quantum key distribution (QKD) [31–37], in which classical information is transmitted over quantum network, and TDMA has been used to generate large entangled cluster states [38]. However, whether more popular classical communication technique such as CDMA [41–44] and OFDMA [39, 40] can be applied to quantum communication systems is still an interesting problem yet to be solved.

---

\*Electronic address: jing-zhang@mail.tsinghua.edu.cn

Recently, various protocols are proposed to extend CDMA to the quantum case [41–44] and there is evidence showing that CDMA can provide higher information rates for quantum communication compared with FDMA [41]. In Ref. [41], particular chaotic phase shifts, which work as the unique code in CDMA, are introduced to spread the information-bearing quantum signals in the frequency regime. Since the chaotic phase shifts introduced for different users are uncorrelated, the cryptographic quantum signals from different users are orthogonal and thus can be distinguished even when we transmit them via the same channel. The cryptographic quantum signals can be decoded by introducing reversed chaotic phase shifts at the receiver side, by which the transmitted quantum information can be recovered coherently. The physical media used in Ref. [41] to transmit quantum information are single-photon lights [43].

Different from the protocol in Ref. [41], instead of single-photon lights, we use bright coherent lights [44] to transmit quantum information over quantum CDMA network, which are easier to be realized in experiments. We find that quantum entanglement can be controllably distributed between two pairs of users sharing a single quantum channel. We also present the particular design of the chaotic phase shifters used in our proposals by introducing electro-optic modulators (EOMs) and chaotic Colpitts oscillator circuits [45] which is not clearly discussed in Ref. [41]. The Pecora-Carrol synchronization technique [46, 47] is introduced to generate the reverse chaotic phase shifts at the receiver side. This paper is organized as follows. In Sec. II, we present the general description of the quantum CDMA network, we use to transmit quantum information. In Sec. III, we state how to distribute maximally-entangled quantum states over proposed quantum CDMA network mediated by bright coherent lights. In Sec. IV, we consider the non-ideal case to see how channel noise will affect our main results. In Sec. V, we present the conclusions and a forecast of future work.

## II. QUANTUM CDMA NETWORK BY CHAOTIC SYNCHRONIZATION

The main purpose of our work is to generate two maximally-entangled states between two pairs of nodes (one pair of nodes are node 1 and node 3 and the second pair of nodes are node 2 and node 4) via a single quantum channel (see Fig. 1). The quantum signals sent by node 1 and node 2 are first encoded by two chaotic phase shifters CPS<sub>1</sub> and CPS<sub>2</sub>, and the two output beams are combined by a 50:50 beam splitter and then transmitted via a quantum channel. At the receiver side, this combined quantum signal is divided into two branches by another 50:50 beam splitter and sent to another two chaotic phase shifters CPS<sub>3</sub> and CPS<sub>4</sub> introduced to decode the information. The recovered quantum signals are then sent to the two receiver nodes.

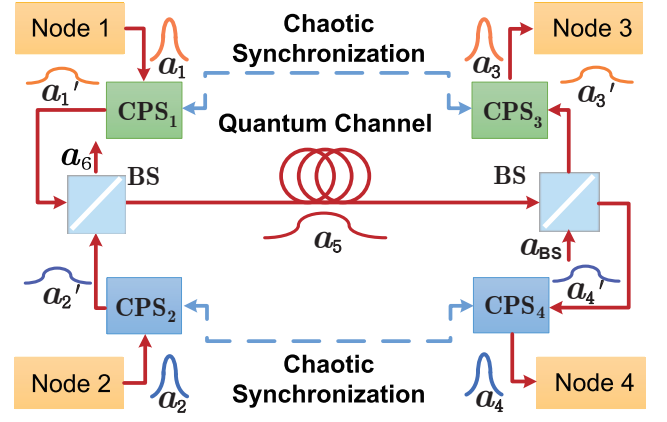


FIG. 1: (color online) Schematic diagram of the quantum CDMA network by chaotic synchronization. The wave packets are broadened by two chaotic phase shifters, i.e., CPS<sub>1</sub> and CPS<sub>2</sub>, at the senders, and then recovered by another two chaotic phase shifters, i.e., CPS<sub>3</sub> and CPS<sub>4</sub>, at the receiver side.

To understand the encoding and decoding processes of our method, let us assume that the optical field entering the  $i$ -th chaotic phase shifter is  $a_i$  ( $i = 1, 2, 3, 4$ ). The chaotic phase shifter CPS<sub>1</sub> (CPS<sub>2</sub>) induces an effective Hamiltonian  $\delta_1(t) a_1^\dagger a_1$  [ $\delta_2(t) a_2^\dagger a_2$ ], where  $\delta_1(t)$  [ $\delta_2(t)$ ] is a classical chaotic signal. It can be shown that CPS<sub>1</sub> (CPS<sub>2</sub>) leads to phase-shift factor  $\exp(-i\theta_1(t))$  [ $\exp(-i\theta_2(t))$ ] for the optical field. At the receiver side, the chaotic phase shifter CPS<sub>3</sub> (CPS<sub>4</sub>) induces an opposite Hamiltonian  $-\delta_1(t) a_3^\dagger a_3$  [ $-\delta_2(t) a_4^\dagger a_4$ ] by which a reversed phase-shift factor  $\exp(i\theta_1(t))$  [ $\exp(i\theta_2(t))$ ] is introduced to decode the information-bearing signal masked by the chaotic phase shift. Here  $\theta_i = \int_0^t \delta_i(t) dt$ ,  $i = 1, 2$ . To assure that the chaotic phase shift at the sender side and that at the receiver side can be exactly cancelled, an auxiliary classical channel between node 1 (node 2) and node 3 (node 4) is introduced to synchronize the two chaotic phase shifters [48, 49] (see Fig. 1).

The whole information transmission process can be represented by the input-output relationship of the whole quantum network from  $a_1, a_2$  to  $a_3, a_4$  (see Fig. 1). To derive it, we can see that the input-output response of the chaotic phase shifters CPS <sub>$i$</sub> ,  $i = 1, 2, 3, 4$  can be written as

$$\begin{aligned} a_1' &= a_1 e^{-i\theta_1}, & a_2' &= a_2 e^{-i\theta_2}, \\ a_3 &= a_3' e^{i\theta_1}, & a_4 &= a_4' e^{i\theta_2}, \end{aligned} \quad (1)$$

and the input-output response of the two beam splitters BS<sub>1</sub> and BS<sub>2</sub> can be written as follows:

BS<sub>1</sub>:

$$a_5 = \frac{1}{\sqrt{2}} a_1' + \frac{1}{\sqrt{2}} a_2', \quad a_6 = \frac{1}{\sqrt{2}} a_1' - \frac{1}{\sqrt{2}} a_2', \quad (2)$$

BS<sub>2</sub>:

$$a'_3 = \frac{1}{\sqrt{2}}a_5 + \frac{1}{\sqrt{2}}a_{BS}, \quad a'_4 = \frac{1}{\sqrt{2}}a_5 - \frac{1}{\sqrt{2}}a_{BS}, \quad (3)$$

Hence, from Eqs. (1-3), we can obtain the input-output relationship of the whole quantum network

$$\begin{aligned} a_3 &= \frac{1}{2}a_1 + \frac{1}{2}a_2e^{i(\theta_1-\theta_2)} + \frac{1}{\sqrt{2}}e^{i\theta_1}a_{BS}, \\ a_4 &= \frac{1}{2}a_2 + \frac{1}{2}a_1e^{i(\theta_2-\theta_1)} - \frac{1}{\sqrt{2}}e^{i\theta_2}a_{BS}. \end{aligned} \quad (4)$$

For the chaotic phase shifts  $\theta_i(t)$ ,  $i = 1, 2$ , we should take average over these broadband “random” phases [50], by which we have:  $\overline{\exp(\pm i\theta_i(t))} \approx \sqrt{M_i}$  [51–53], where

$$M_i = \exp \left[ -\pi \int_{\omega_{li}}^{\omega_{ui}} d\omega S_{\delta_i}(\omega) / \omega^2 \right]. \quad (5)$$

$S_{\delta_i}(\omega)$  is the power spectrum density of the signal  $\delta_i(t)$  and  $\omega_{li}$ ,  $\omega_{ui}$  are the “lower” and “upper” bounds of the frequency band of  $\delta_i(t)$ , respectively. Equation (4) can then be reduced to

$$\begin{aligned} a_3 &= \frac{1}{2}a_1 + \frac{\sqrt{M_1M_2}}{2}a_2 + \sqrt{\frac{M_1}{2}}a_{BS}, \\ a_4 &= \frac{1}{2}a_2 + \frac{\sqrt{M_1M_2}}{2}a_1 - \sqrt{\frac{M_2}{2}}a_{BS}. \end{aligned} \quad (6)$$

The correction factor  $M_i$  may become extremely small when  $\delta_i(t)$  is induced by a chaotic signal which has a broadband frequency spectrum. Thus we have  $a_3 \approx a_1/2$ ,  $a_4 \approx a_2/2$ , which means that the quantum signal transmitted from node 1 to node 3 and the quantum signal transmitted from node 2 to node 4 can be totally decoupled from each other although they are transmitted simultaneously on the same quantum channel. The mechanism of such a quantum multiple access network is that the information bearing fields transmitted on the quantum channel are broadened by the chaotic phase shifters in the frequency regime, which cannot be detected unless we can reduce the chaotic phase shifts and sharpen the quantum signal by chaotic synchronization. This idea is quite similar to the classical CDMA communication. That is why we call it quantum CDMA network in Ref. [41].

Now, let us consider the case where the quantum fields  $a_1$  and  $a_2$  are in the coherent states  $|\alpha_1\rangle$  and  $|\alpha_2\rangle$ , and the field  $a_{BS}$  is in a vacuum state. It can be easily checked from the input-output relationship given by Eq. (6) that the output fields  $a_3$  and  $a_4$  of the quantum network are in the coherent states

$$\begin{aligned} |\alpha_3\rangle &= \left| \frac{1}{2}\alpha_1 + \frac{1}{2}\sqrt{M_1M_2}\alpha_2 \right\rangle \approx \left| \frac{1}{2}\alpha_1 \right\rangle, \\ |\alpha_4\rangle &= \left| \frac{1}{2}\alpha_2 + \frac{1}{2}\sqrt{M_1M_2}\alpha_1 \right\rangle \approx \left| \frac{1}{2}\alpha_2 \right\rangle. \end{aligned} \quad (7)$$

### III. QUANTUM ENTANGLEMENT DISTRIBUTION OVER Q-CDMA NETWORK

Let us then consider how to distribute two-qubit quantum entanglement over the quantum CDMA network. In our proposal, the qubit states are stored in the dark states of four  $\Lambda$ -type three-level atoms in four optical cavities (see Fig. 2). What we want to do is to generate maximally-entangled state between atom 1 (atom 2) and atom 3 (atom 4). Here we extend the strategy in Refs. [54, 55] to generate such kinds of distributed entangled states by bright coherent lights. The Hamiltonian of the  $i$ -th coupled atom-cavity system can be expressed as

$$\tilde{H}_i^{qc} = \omega_c a_i^\dagger a_i + \frac{\omega_q}{2} \sigma_z^{(i)} + g \left( a_i^\dagger \sigma_-^{(i)} + a_i \sigma_+^{(i)} \right), \quad (8)$$

where  $\omega_c$ ,  $a_i$  ( $a_i^\dagger$ ) are the frequency and the annihilation (creation) operator of the cavity mode;  $\omega_q$ ,  $\sigma_z^{(i)}$  and  $\sigma_\pm^{(i)}$  are the frequency, the z-axis Pauli operator, and the ladder operators of the qubit; and  $g$  is the coupling strength between the qubit and the cavity mode. Here, to simplify the discussion, we have assumed that the system parameters are the same for four qubit-cavity systems. Under the dispersive-detuning condition  $|\Delta| = |\omega_c - \omega_q| \gg |g|$ , the Hamiltonian can be diagonalized and reexpressed in the interaction picture as [56]

$$H_i^{qc} = \frac{g^2}{\Delta} a_i^\dagger a_i \sigma_z^{(i)}. \quad (9)$$

In this paper, we introduce four electro-optic modulators (EOMs) [57] acting as the chaotic phase shifters  $CPS_i$ . It is known that the refractive index of the electro-optic crystal in EOM can be varied by changing the voltage  $V(t)$  acting on it (see Fig. 3(a)). Based on this effect, we let the information-bearing optical field pass through the EOM to obtain a phase shift  $\beta$  which will be changed by varying the voltage  $V(t)$  acting on it. This phase shift can be expressed as  $\beta = [(\omega n^3 r L) / (cd)] V(t)$ , where  $\omega$  is the frequency of the injected light.  $n$  are the refractive index and the electro-optic coefficient of the electro-optic crystal in EOM.  $L$  and  $d$  are respectively the length and thickness of the EOM (see Fig. 3(a)).  $c$  is the velocity of light. Therefore, when the optical field transmits through the EOM, an interaction Hamiltonian  $H_i = \delta_i(t) a_i^\dagger a_i = -(\hbar/\tau) \beta a_i^\dagger a_i$  [58] can be obtained, where  $a_i$  ( $a_i^\dagger$ ) is the annihilation (creation) operator of the injected field and  $\tau$  is the optical round-trip time through the EOM. In present system, each pair of EOMs is driven by two synchronized standard Colpitts oscillator circuits, as shown in Fig. 3(b), and the specific synchronized circuit is presented in Appendix. We use the voltage  $V_{C2}$  to drive the EOM at the sender side, and the voltage  $\tilde{V}_{C2}$  to drive another EOM at the receiver side, as shown in Fig. 3(b).

To show how the quantum entanglement is distributed over our quantum CDMA network, we assume

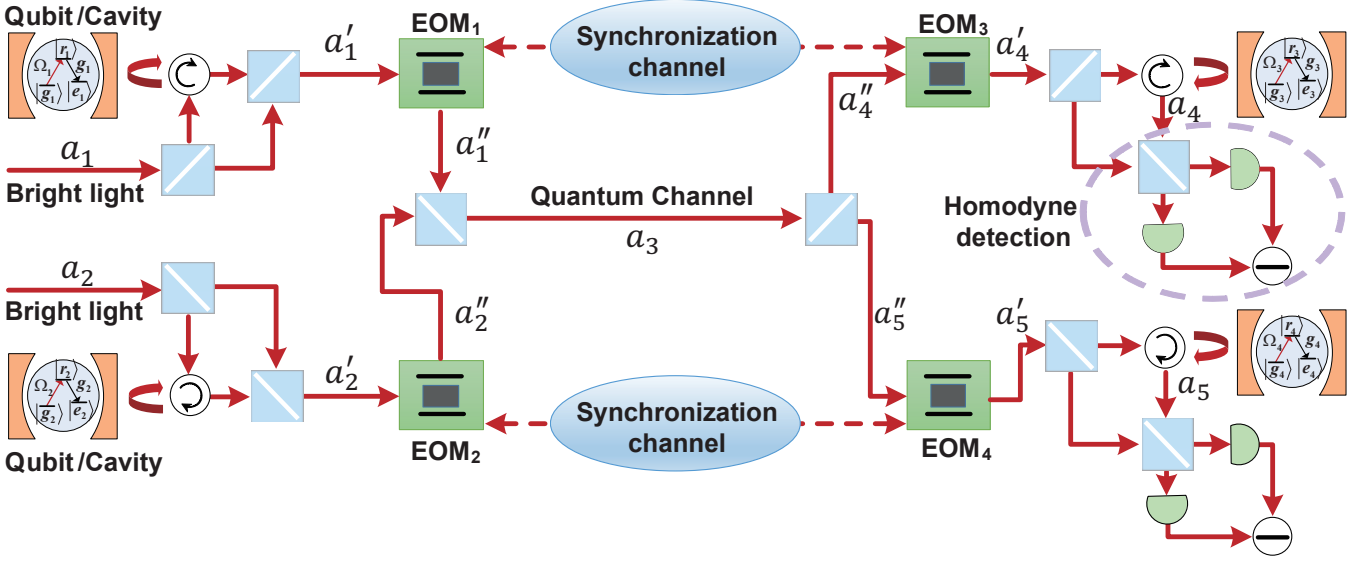


FIG. 2: (color online) Schematic diagram of the entanglement distribution over a quantum multiple-access network. The bright coherent lights are sent to two cavities 1 and 2 in which the optical fields interact with the atoms 1 and 2, respectively. After that, the two output beams transmit through two EOMs, i.e., EOM<sub>1</sub> and EOM<sub>2</sub>, and are broadened in the frequency domain. The two output beams are then combined by an beam splitter and transmitted through a single quantum channel. At the receiver side, the combined optical field is split into two branches by another beam splitter and fed into another two EOMs, i.e., EOM<sub>3</sub> and EOM<sub>4</sub>. Since the chaotic circuits driving EOM<sub>1</sub> (EOM<sub>2</sub>) and EOM<sub>3</sub> (EOM<sub>4</sub>) are synchronized, the chaotic phases introduced at the sender side can be compensated at the receiver side, and thus the quantum signals transmitted can be recovered. The recovered quantum signals are then stored in the dark states of the atoms 3 and 4, and homodyne detections are preformed for the output fields to post-select the maximally entangled states.

that the  $i$ -th atom is in a superposition state  $|\psi_i\rangle = (|g_i\rangle + |e_i\rangle)/\sqrt{2}$  ( $i = 1, 2, 3, 4$ ). The probe field entering the cavity 1 (cavity 2) is a bright coherent light  $|\alpha\rangle$  with average photon number  $\bar{n} = |\alpha|^2 \gg 1$ . When the probe field comes out of cavity 1 (cavity 2) at time  $\tau'$ , the system composed of the atom 1 and the probe field fed out of cavity 1 is in an entangled state

$$e^{-iH_1^{qc}\tau'}|\psi_1\rangle|\alpha\rangle = \frac{1}{\sqrt{2}} \left( |g_1\rangle|\alpha e^{-i\phi/2}\rangle + |e_1\rangle|\alpha e^{i\phi/2}\rangle \right). \quad (10)$$

Similarly, the system composed of the atom 2 and the probe light fed out of cavity 2 is also in an entangled state

$$e^{-iH_2^{qc}\tau'}|\psi_2\rangle|\alpha\rangle = \frac{1}{\sqrt{2}} \left( |g_2\rangle|\alpha e^{-i\phi/2}\rangle + |e_2\rangle|\alpha e^{i\phi/2}\rangle \right). \quad (11)$$

Here,  $H_1^{qc}$ ,  $H_2^{qc}$  are the Hamiltonians given by Eq. (9) and  $\phi = 2g^2\tau'/\Delta$  is the phase shift of the probe field induced by the qubit-cavity coupling. Thus, the system composed of atoms 1, 2 and the two probe lights before entering our q-CDMA network is in a separable state

$$\frac{1}{2} \left[ |g_1g_2\rangle|\alpha e^{-i\phi/2}\rangle|\alpha e^{-i\phi/2}\rangle + |e_1g_2\rangle|\alpha e^{i\phi/2}\rangle|\alpha e^{-i\phi/2}\rangle \right. \\ \left. + |g_1e_2\rangle|\alpha e^{-i\phi/2}\rangle|\alpha e^{i\phi/2}\rangle + |e_1e_2\rangle|\alpha e^{i\phi/2}\rangle|\alpha e^{i\phi/2}\rangle \right].$$

From Eq. (7), the system composed of the atoms 1 and 2 and those two probe fields which enter the cavities 3 and

4 is in the state

$$|\Phi\rangle = \left( \frac{1}{\sqrt{2}}|g_1\rangle \left| \frac{1}{2}\alpha e^{-i\phi/2} \right\rangle + \frac{1}{\sqrt{2}}|e_1\rangle \left| \frac{1}{2}\alpha e^{i\phi/2} \right\rangle \right) \\ \left( \frac{1}{\sqrt{2}}|g_2\rangle \left| \frac{1}{2}\alpha e^{-i\phi/2} \right\rangle + \frac{1}{\sqrt{2}}|e_2\rangle \left| \frac{1}{2}\alpha e^{i\phi/2} \right\rangle \right).$$

Here we have omitted those  $\sqrt{M_1M_2}$  terms since the factors  $M_1$  and  $M_2$  are negligibly small in the chaotic regime. After transmitting over the quantum CDMA network, the probe fields  $a_3$  and  $a_4$  interact with the atoms 3 and 4, and the interaction times are both  $\tau'$ . Thus, the state of the total system composed of the four atoms and the optical fields fed out of the quantum network is

$$e^{-i(H_3^{qc}+H_4^{qc})\tau'}|\Phi\rangle \frac{1}{2} (|g_3\rangle + |e_3\rangle)(|g_4\rangle + |e_4\rangle) \\ = \left( \frac{1}{\sqrt{2}}|\Psi_{13}^+\rangle \left| \frac{1}{2}\alpha \right\rangle + \frac{1}{2}|g_1g_3\rangle \left| \frac{1}{2}\alpha e^{-i\phi} \right\rangle \right. \\ \left. + \frac{1}{2}|e_1e_3\rangle \left| \frac{1}{2}\alpha e^{i\phi} \right\rangle \right) \\ \left( \frac{1}{\sqrt{2}}|\Psi_{24}^+\rangle \left| \frac{1}{2}\alpha \right\rangle + \frac{1}{2}|g_2g_4\rangle \left| \frac{1}{2}\alpha e^{-i\phi} \right\rangle \right. \\ \left. + \frac{1}{2}|e_2e_4\rangle \left| \frac{1}{2}\alpha e^{i\phi} \right\rangle \right), \quad (12)$$

where  $|\Psi_{13}^+\rangle = (|g_1e_3\rangle + |e_1g_3\rangle)/\sqrt{2}$  is the maximally-



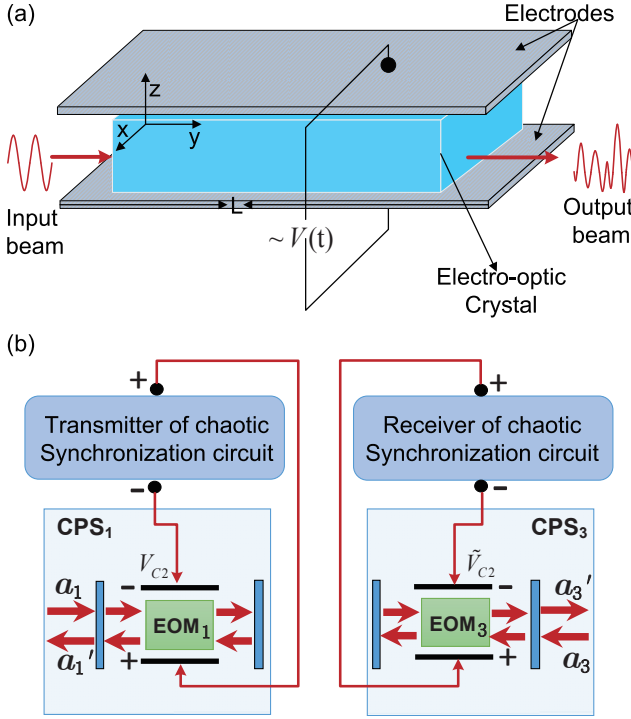


FIG. 3: (color online) (a) Schematic diagram of a transverse electro-optic modulator. The voltage is applied perpendicular to the propagational direction of the input beam, and the refractive index of the electro-optic crystal can be changed by varying the voltage  $V$ , which induces a voltage-dependent phase shift on the input beam; (b) The diagram of the chaotic synchronization circuit between  $\text{CPS}_1$  and  $\text{CPS}_3$ , where the transmitter drives the  $\text{EOM}_1$  and the receiver drives the  $\text{EOM}_3$ .

entangled state between atom 1 and atom 3 and  $|\Psi_{24}^+\rangle = (|g_2e_4\rangle + |e_2g_4\rangle)/\sqrt{2}$  is the maximally-entangled state between atom 2 and atom 4.

Finally, we impose homodyne detections on the probe fields leaking out of the cavities 3 and 4. As shown in Eq. (12), the state of the probe fields leaking out of the cavities 3 and 4 can be three possible states  $|\alpha/2\rangle$ ,  $|\alpha e^{-i\phi}/2\rangle$ , and  $|\alpha e^{i\phi}/2\rangle$ . Since the probe fields are bright coherent lights with average photon number  $\bar{n} = |\alpha|^2 \gg 1$ , we have

$$\begin{aligned} \left| \left\langle \frac{1}{2}\alpha \left| \frac{1}{2}\alpha e^{-i\phi} \right\rangle \right|^2 &= \exp[-\bar{n} \sin^2(\phi/2)] \approx 0, \\ \left| \left\langle \frac{1}{2}\alpha \left| \frac{1}{2}\alpha e^{i\phi} \right\rangle \right|^2 &= \exp[-\bar{n} \sin^2(\phi/2)] \approx 0, \\ \left| \left\langle \frac{1}{2}\alpha e^{-i\phi} \left| \frac{1}{2}\alpha e^{i\phi} \right\rangle \right|^2 &= \exp(-\bar{n} \sin^2 \phi) \approx 0, \end{aligned}$$

which means that the three coherent states  $|\alpha/2\rangle$ ,  $|\alpha e^{-i\phi}/2\rangle$ , and  $|\alpha e^{i\phi}/2\rangle$  are pairwise orthogonal and thus completely distinguishable. Thus, the homodyne detections on the probe fields are just projective measurements. Corresponding to the three measurement outputs

$\alpha/2$ ,  $\alpha e^{-i\phi}/2$  and  $\alpha e^{i\phi}/2$ , the states of the system composed of atom 1 and 3 (atom 2 and atom 4) collapse to the maximally-entangled state  $|\Psi_{13}^+\rangle$  ( $|\Psi_{24}^+\rangle$ ) and two separable states  $|g_1g_3\rangle$  ( $|g_2g_4\rangle$ ) and  $|e_1e_3\rangle$  ( $|e_2e_4\rangle$ ). The most important case is that the measurement outputs of the probe fields leaking out of the cavity 3 and cavity 4 are both  $\alpha/2$ . In this case, the atoms 1 and 3 are in the maximally-entangled state  $|\Psi_{13}^+\rangle$  and the atoms 2 and 4 are in the maximally-entangled state  $|\Psi_{24}^+\rangle$ , which means that we generate two maximally-entangled states between two pairs of nodes by sharing the same quantum channel.

We then consider the interference effects between the quantum signals from the two pairs of users. These interference effects have been omitted in our previous discussions under the condition that the correction factor  $M$  ( $M = M_1 M_2$ ) is negligibly small if the chaotic phases introduced have very broad bandwidths. However, these interference effects will affect the information transmission process if the bandwidths of the phase signals are not broad enough. To show this, let us consider how the correction factors  $M_1$  and  $M_2$  will change if we tune the correspondent bandwidths of the chaotic signals  $\delta_1$  and  $\delta_2$ . From Fig. 4(a), we can see that both  $M_1$  and  $M_2$  decrease with the increase of the bandwidth of  $\delta_1$  and  $\delta_2$ , and when we take the bandwidth values of the chaotic signals as 450 MHz,  $M_1$  and  $M_2$  are 0.0012 and 0.0033, respectively. With experimental realizable parameters of the Colpitts chaotic circuits [46, 47], it is not quite difficult to generate a chaotic phase with bandwidth of 500 MHz, and thus  $M_1$  and  $M_2$  can be very small. In the meanwhile, we choose the average photon number  $\bar{n} = 10$ , and thus we have  $M_1 M_2 \ll 4/\bar{n}$ . This makes it reasonable to omit the  $\sqrt{M_1 M_2}$  terms in Eqs. (6), (7), and (14). In order to check whether the phase shifts induced by the phase shifters are in the chaotic regime, we show in Fig. 4(b) the Lyapunov exponents of Colpitts circuits with different bandwidths. When the bandwidths of the Colpitts circuits are smaller than 100 MHz, the Lyapunov exponents of the Colpitts circuits are equal 0, which means that these circuits work in the periodic regime. If we increase the bandwidths of the circuits, the Colpitts circuits will then enter the chaotic regime if the bandwidths are larger than 100 MHz which corresponds to positive Lyapunov exponents (see Fig. 4(b)). This is also confirmed by the phase diagrams and the power spectra of the circuits with bandwidth of 100 MHz shown in Figs. 4(c) and (d), and those of the circuits with bandwidth of 500 MHz in Figs. 4(e) and (f).

In order to show the efficiency of entanglement distribution by the quantum CDMA network, we show in Fig. 5 the fidelities  $F_1 = \langle \Psi_{13}^+ | \rho_{13} | \Psi_{13}^+ \rangle$  and  $F_2 = \langle \Psi_{24}^+ | \rho_{24} | \Psi_{24}^+ \rangle$  versus the bandwidths of the chaotic signals and the average photon number of the probe fields  $\bar{n}$ , where  $|\Psi_{13}^+\rangle$  ( $|\Psi_{24}^+\rangle$ ) is the desired maximally-entangled state between atoms 1 and 3 (atoms 2 and 4); and  $\rho_{13}$  ( $\rho_{24}$ ) is the real state of the atoms 1 and 3 (atoms 2 and 4). In our simulations, we take  $\phi = \pi/3$ , where  $\phi$  is

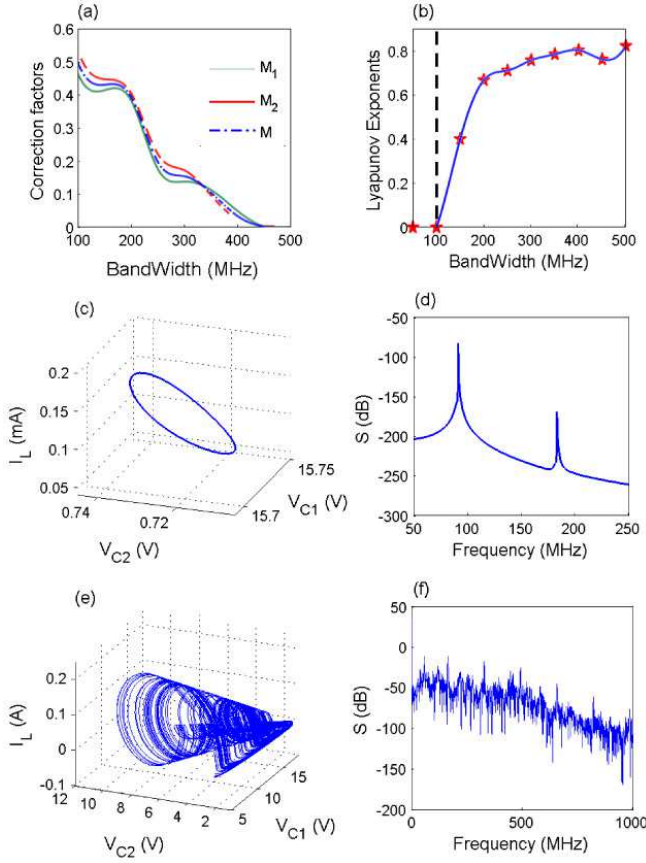


FIG. 4: (color online) (a) The factors  $M_1$ ,  $M_2$ , and  $M$  versus the bandwidths of the Colitts circuits without channel noise. The green solid curve represents the factor  $M_1$ . The red dashed line denotes the curve for the factor  $M_2$ . The blue dash-dot curve shows the factor  $M = \sqrt{M_1 M_2}$ . (b) The Lyapunov exponents of the Colpitts circuits versus different bandwidths of the circuits. (c), (d) are the phase diagram and the power spectrum of the Colpitts circuit with bandwidth 100 MHz, and (e), (f) correspond to the phase diagram and the power spectrum of the Colpitts circuit with bandwidth of 500 MHz.

the phase shift of the probe fields induced by the qubit-cavity coupling. The trajectories of the fidelity  $F_1$  versus the correction factor  $M$  and the average photon number  $\bar{n}$  are given in Fig. 5(a). We can see clearly that the fidelity  $F_1$  can be very high if the factor  $M$  is small enough and  $\bar{n}$  is not too small which corresponds to our previous analysis. If we fix  $\bar{n} = 10$  and increase the bandwidth of the signals, we can see the increase of the fidelities  $F_1$  and  $F_2$  as desired (see Fig. 5(b)). Both  $F_1$  and  $F_2$  grow very quickly to approach 1 with the increase of the bandwidths of the signals to be larger than 400 MHz, which corresponds to a perfect entanglement distribution.

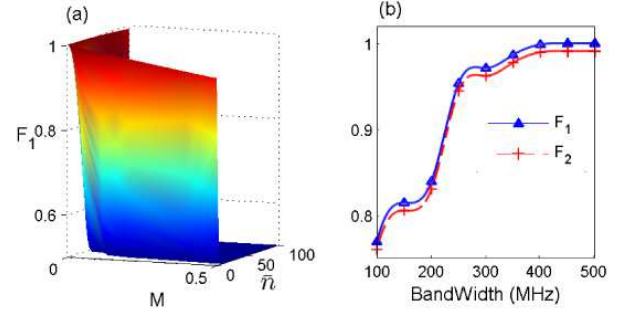


FIG. 5: (color online) (a) Fidelity  $F_1$  versus different values of the correction factor  $M$  and the average photon number  $\bar{n}$ . (b) Trajectories of the fidelities  $F_1$  and  $F_2$  versus different bandwidths of the signals. Both  $F_1$  and  $F_2$  can be very close to the ideal case, i.e.,  $F_1, F_2 \approx 1$  when the bandwidth of the signal is larger than 400 MHz, which means that we efficiently suppress the interference effects of our quantum CDMA network induced by the crosstalk between different data streams.

#### IV. NONIDEAL CASE: EFFECTS OF THE CHANNEL NOISE

In the previous sections, we consider the ideal case in which the channel noises are omitted. To show the efficiency of our method in more practical case, we consider the effects of the channel noises in this section [59, 60]. The channel noises in quantum communication may come from different sources, such as the vibration of the optical fiber used for transmitting quantum signals. Most of the channel noises, especially those induced by the fibers, are low-frequency noises with several to several hundreds of kHz, which is far smaller than the characteristic frequency of the information-bearing fields, and also smaller than the frequency band of the chaotic phase shifts introduced by the chaotic circuits which is typically of several hundreds MHz. For these reasons, we can omit the dynamical processes of the channel noises and simply believe that they act as a beam splitter to extract energy of the information-bearing field (see Fig. 6). As shown in Fig. 6, the input-output relationship of the beamsplitter  $BS_3$  used to represent the effects of the channel noises can be written as

$$a_7 = \sqrt{1 - \eta} a_5 + \sqrt{\eta} a_{NS}, \quad a_8 = \sqrt{1 - \eta} a_5 - \sqrt{\eta} a_{NS}, \quad (13)$$

where  $a_{NS}$  represents the noise mode and  $\eta$  denotes the decay rate induced by the noise. From Eqs. (1) to (6) and Eq. (13), we can obtain the input-output relationship of

the noisy quantum CDMA network as

$$\begin{aligned}
 a_3 &= \frac{\sqrt{1-\eta}}{2}a_1 + \frac{\sqrt{(1-\eta)M_1M_2}}{2}a_2 + \sqrt{\frac{\eta M_1}{2}}a_{\text{NS}} \\
 &\quad + \sqrt{\frac{M_1}{2}}a_{\text{BS}}, \\
 a_4 &= \frac{\sqrt{1-\eta}}{2}a_2 + \frac{\sqrt{(1-\eta)M_1M_2}}{2}a_1 + \sqrt{\frac{\eta M_2}{2}}a_{\text{NS}} \\
 &\quad - \sqrt{\frac{M_2}{2}}a_{\text{BS}}.
 \end{aligned}$$

If we further assume that the field  $a_{\text{NS}}$  is in a vacuum state, the output fields of the quantum CDMA network, i.e.,  $a_3$  and  $a_4$ , are in the following coherent states

$$\begin{aligned}
 |\alpha_3\rangle &= \left| \frac{\sqrt{1-\eta}}{2}\alpha_1 + \frac{\sqrt{(1-\eta)M_1M_2}}{2}\alpha_2 \right\rangle, \\
 |\alpha_4\rangle &= \left| \frac{\sqrt{1-\eta}}{2}\alpha_2 + \frac{\sqrt{(1-\eta)M_1M_2}}{2}\alpha_1 \right\rangle. \quad (14)
 \end{aligned}$$

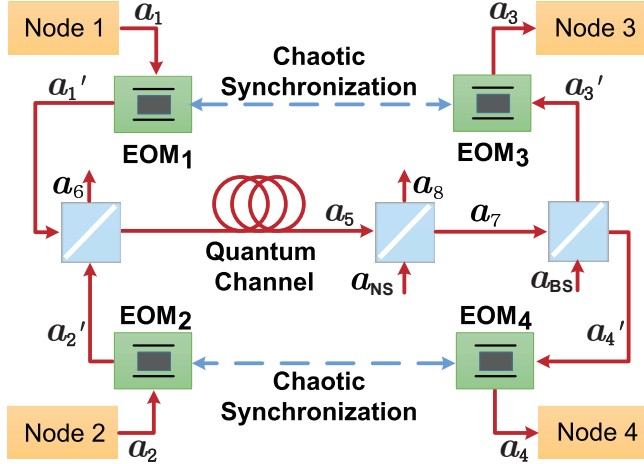


FIG. 6: (color online) Schematic diagram of quantum CDMA network contains channel noise, where we use the beamsplitter  $\text{BS}_3$  to introduce channel noise.

Recall that the  $i$ -th atom is in the superposition state  $|\psi_i\rangle = (|g_i\rangle + |e_i\rangle)/\sqrt{2}$ , and the probe field entering the cavity 1 (cavity 2) is a bright coherent light  $|\alpha\rangle$  with average photon number  $\bar{n} = |\alpha|^2 \gg 1$ . By omitting the terms related to  $\sqrt{M_1M_2}$  in Eq. (14), we can easily obtain the state of the total system composed of the four atoms and output fields of the quantum network as

$$\begin{aligned}
 |\Psi\rangle &= \left( \frac{1}{\sqrt{2}}|\Psi_{13}^+\rangle \left| \frac{\sqrt{1-\eta}}{2}\alpha \right\rangle + \frac{1}{2}|g_1g_3\rangle \left| \frac{\sqrt{1-\eta}}{2}\alpha e^{-i\phi} \right\rangle \right. \\
 &\quad \left. + \frac{1}{2}|e_1e_3\rangle \left| \frac{\sqrt{1-\eta}}{2}\alpha e^{i\phi} \right\rangle \right) \\
 &\quad \left( \frac{1}{\sqrt{2}}|\Psi_{24}^+\rangle \left| \frac{\sqrt{1-\eta}}{2}\alpha \right\rangle + \frac{1}{2}|g_2g_4\rangle \left| \frac{\sqrt{1-\eta}}{2}\alpha e^{-i\phi} \right\rangle \right. \\
 &\quad \left. + \frac{1}{2}|e_2e_4\rangle \left| \frac{\sqrt{1-\eta}}{2}\alpha e^{i\phi} \right\rangle \right).
 \end{aligned}$$

If the decay rate  $\eta$  induced by the channel noise is not quite high and the probe fields are bright enough with average photon number  $\bar{n} = |\alpha|^2 \gg 1/(1-\eta)$ , we have

$$\begin{aligned}
 \left| \left\langle \frac{\sqrt{1-\eta}}{2}\alpha \left| \frac{\sqrt{1-\eta}}{2}\alpha e^{-i\phi} \right\rangle \right|^2 &= e^{-(1-\eta)\bar{n}\sin^2(\phi/2)} \approx 0, \\
 \left| \left\langle \frac{\sqrt{1-\eta}}{2}\alpha \left| \frac{\sqrt{1-\eta}}{2}\alpha e^{i\phi} \right\rangle \right|^2 &= e^{-(1-\eta)\bar{n}\sin^2(\phi/2)} \approx 0, \\
 \left| \left\langle \frac{\sqrt{1-\eta}}{2}\alpha e^{-i\phi} \left| \frac{\sqrt{1-\eta}}{2}\alpha e^{i\phi} \right\rangle \right|^2 &= e^{-(1-\eta)\bar{n}\sin^2\phi} \approx 0,
 \end{aligned}$$

which means that the three coherent states  $|\sqrt{1-\eta}\alpha/2\rangle$ ,  $|\sqrt{1-\eta}\alpha e^{-i\phi}/2\rangle$ , and  $|\sqrt{1-\eta}\alpha e^{i\phi}/2\rangle$  are pairwise orthogonal and thus completely distinguishable. Thus we can impose homodyne detections on the fields leaking out of the cavities 3 and 4. If the corresponding measurement outputs for the two probe fields are both  $\sqrt{1-\eta}\alpha/2$ , the state of atoms 1 and 3 will collapse to the maximally-entangled states  $|\Psi_{13}^+\rangle$  and that of the atoms 2 and 4 will collapse to the maximally-entangled states  $|\Psi_{24}^+\rangle$ . From the above discussions, we can conclude that our method is still valid if only the decay rate induced by the channel noise is not quite high such that the decayed probe fields are still bright enough.

However, if the decay rate  $\eta$  induced by the channel noises are too high such that the average photon number  $\bar{n} = |\alpha|^2$  is comparable to  $1/(1-\eta)$ , our entanglement distribution strategy will not be so perfect. In this case, we need to analyze the influence of noise on the fidelities  $F_1$  and  $F_2$ . Without loss of generality, let us focus on the fidelity  $F_1 = \langle \Psi_{13}^+ | \rho_{13} | \Psi_{13}^+ \rangle$  versus different decay rate  $\eta$  and average photon number  $\bar{n}$ . The discussion for the fidelity  $F_2$  are quite similar and thus is omitted. We still choose  $\phi = \pi/3$  and assume that the correction factors  $M_1 = M_2 \approx 0$ . With these system parameters, we show in Fig. 7 how the decay rate  $\eta$  affects the entanglement distribution. As can be seen from Fig. 7(a), fidelity  $F_1$  can be very high when  $\eta$  is small and the average photon number is not large. Figure 7(b) shows the curves of the fidelity  $F_1$  versus  $\eta$  for several different cases. The red solid curve represent the ideal case, i.e.,  $F_1 = 1$ , which means that atoms 1 and 3 are in the maximally-entangled state. The black dashed curve with plus signs denotes the trajectory of the fidelity  $F_1$  with increasing  $\eta$  ranging from 0 to 1. The blue asterisks dash-dot curve shows the fidelity  $F_1$  versus  $\eta$  without the four EOMs in our quantum CDMA network. By comparing these three curves, we can see that the fidelity  $F_1$  will be greatly decreased if we move away the four EOMs in our quantum CDMA network. In the meanwhile, with EOMs, we can obtain a very high fidelity when the decay rate  $\eta$  is not too high.

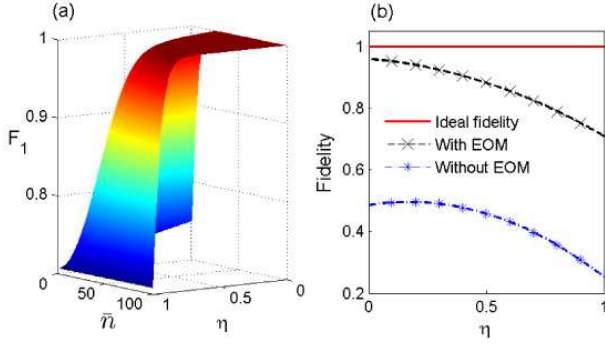


FIG. 7: (color online) (a) Fidelity  $F_1$  versus different decay rates  $\eta$  and the average photon number  $\bar{n}$ . (b) Trajectories of  $F_1$  versus  $\eta$  with fixed  $\bar{n} = 10$ . The black dashed curve with plus signs shows the curve of the fidelity  $F_1$  realized by our quantum CDMA network. The blue asterisks dash-dot curve represents the curve of  $F_1$  when we the four EOMs are moved away. It is shown that our strategy can still be valid when we consider the channel noise if only the decay rate induced by the channel noises is not too high.

## V. CONCLUSIONS

In summary, we present a strategy to distribute quantum entanglement between two pairs of users via a single quantum channel. The interference of the quantum signals from different senders are greatly suppressed by introducing chaotic phase shifts to broaden the quantum signals in the frequency domain. It is shown that the two maximally-entangled states can be generated between two pairs of nodes even when we consider the channel noises. Our strategy is also hopeful to be applied to other systems such as solid-state quantum circuits, and it also provides new perspectives for the field of quantum network control.

## ACKNOWLEDGMENTS

CLZ would like to thank Dr. R. B. Wu for helpful discussions. JZ and YXL are supported by the National Basic Research Program of China (973 Program) under Grant No. 2014CB921401, the Tsinghua University Initiative Scientific Research Program, and the Tsinghua National Laboratory for Information Science and

Technology (TNList) Cross-discipline Foundation. JZ is supported by the NSFC under Grant Nos. 61174084, 61134008. YXL is supported by the NSFC under Grant Nos. 10975080, 61025022, 91321208. FN is partially supported by the RIKEN iTHES Project, MURI Center for Dynamic Magneto-Optics, Grant-in-Aid for Scientific Research (A).

## APPENDIX: CHAOTIC SYNCHRONIZATION OF COLPITTS OSCILLATOR CIRCUITS

In the system we consider, each pair of EOMs is driven by two standard chaotic Colpitts oscillator circuits [45], which are synchronized by the Pecora-Carroll synchronization strategy [46, 47], as shown in Fig. 8. The Colpitts chaotic synchronization circuit comprises of a transmitter and a receiver. The transmitter is a standard Colpitts oscillator circuit, which will enter the chaotic regime for particular system parameters. The receiver is a part of the standard Colpitts oscillator circuit. In our design, the system parameters of the Colpitts oscillator circuits, such as the resistance  $R$ , the inductance  $L$ , the capacitances  $C_1$  and  $C_2$ , and the voltage  $V_{CC}$ , are chosen as  $R = 27.99 \, \Omega$ ,  $L = 17.5 \, \text{nH}$ ,  $C_1 = 13.1 \, \text{pF}$ ,  $C_2 = 12.7 \, \text{pF}$ , and  $V_{CC} = 15 \, \text{V}$ , under which the synchronized voltages  $V_{C2}$  and  $\tilde{V}_{C2}$  are broadband chaotic signals with bandwidths of 500 MHz [46, 47].

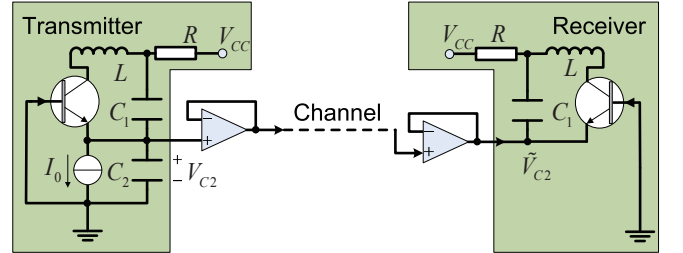


FIG. 8: (color online) Schematic diagram of the synchronized chaotic Colpitts circuits which is composed of a transmitter and a receiver. Here we adopt the Pecora-Carroll synchronization strategy to synchronize the two chaotic Colpitts circuits [48].

[1] M. D. Lukin, Trapping and Manipulating Photon States in Atomic Ensembles, *Rev. Mod. Phys.* **75**, 457 (2003).  
[2] L.-M. Duan and C. Monroe, Quantum Networks with Trapped Ions, *Rev. Mod. Phys.* **82**, 1209 (2010).  
[3] N. Sangouard, C. Simon, H. de Riedmatten, and N. Gisin, Quantum Repeaters Based on Atomic Ensembles and Linear Optics, *Rev. Mod. Phys.* **83**, 33 (2011).  
[4] J. Q. You and F. Nori, Superconducting Circuits and Quantum Information, *Physics Today* **58**, 42 (2005).  
[5] Y. Makhlin, G. Schön, and A. Shnirman, Quantum-state

Engineering with Josephson-junction Devices, *Rev. Mod. Phys.* **73**, 357 (2001).  
[6] Z. L. Xiang, S. Ashhab, J. Q. You, and F. Nori, Hybrid Quantum Circuits: Superconducting Circuits Interacting with Other Quantum Systems, *Rev. Mod. Phys.* **85**, 623 (2013).  
[7] H. J. Kimble, The Quantum Internet, *Nature* **453**, 1023 (2008).  
[8] M. A. Sillanpää, J. I. Park, and R. W. Simmonds, Coherent Quantum State Storage and Transfer Between Two



- Phase Qubits via a Resonant Cavity, *Nature* **449**, 438 (2007).
- [9] X.-B. Wang, T. Hiroshima, A. Tomita, and M. Hayashi, *Phys. Rep.* **448**, 1 (2007).
  - [10] J.-W. Pan, Z.-B. Chen, C.-Y. Lu, H. Weinfurter, A. Zeilinger, and M. Zukowski, Multi-photon Entanglement and Interferometry, *Rev. Mod. Phys.* **84** 777 (2012).
  - [11] N. Gisin, G. Ribordy, W. Tittel, and H. Zbinden, Quantum cryptography, *Rev. Mod. Phys.* **74**, 145 (2002).
  - [12] M. Razavi, Multiple-Access Quantum Key Distribution Networks, *IEEE Trans. Commun.* **60**, 3071 (2012).
  - [13] J. I. Cirac, P. Zoller, H. J. Kimble, and H. Mabuchi, Quantum State Transfer, and Entanglement Distribution among Distant Nodes in a Quantum Network, *Phys. Rev. Lett.* **78**, 3221 (1997).
  - [14] X. Maitre, E. Hagley, G. Nogues, C. Wunderlich, P. Goy, M. Brune, J. M. Raimond, and S. Haroche, Quantum Memory with a Single Photon in a Cavity, *Phys. Rev. Lett.* **79**, 769 (1997).
  - [15] D. F. Phillips, A. Fleischhauer, A. Mair, R. L. Walsworth, and M. D. Lukin, Storage of Light in Atomic Vapor, *Phys. Rev. Lett.* **86**, 783 (2001).
  - [16] L. M. Duan, M. D. Lukin, J. I. Cirac, and P. Zoller, Long-distance Quantum Communication with Atomic Ensembles and Linear Optics, *Nature* **414**, 41 (2001).
  - [17] D. N. Matsukevich and A. Kuzmich, Quantum State Transfer Between Matter and Light, *Science* **306**, 663 (2004).
  - [18] A. Acín, J. I. Cirac, and M. Lewenstein, Entanglement percolation in quantum networks, *Nature Phys.* **3**, 256 (2007).
  - [19] X.-Y. Lü, J.-B. Liu, C.-L. Ding, and J.-H. Li, Dispersive Atom-field Interaction Scheme for Three-dimensional Entanglement Between Two Spatially Separated Atoms, *Phys. Rev. A* **78**, 032305 (2008).
  - [20] D. Felinto, C. W. Chou, J. Laurat, E. W. Schomburg, H. de Riedmatten, and H. J. Kimble, Conditional Control of the Quantum States of Remote Atomic Memories for Quantum Networking, *Nature Phys.* **2**, 844 (2006).
  - [21] C. H. van der Wal, M. D. Eisaman, A. Andre, R. L. Walsworth, D. F. Phillips, A. S. Zibrov, M. D. Lukin, Atomic Memory for Correlated Photon States, *Science* **301**, 196 (2003).
  - [22] C.-W. Chou, J. Laurat, H. Deng, K. S. Choi, H. de Riedmatten, D. Felinto, and H. J. Kimble, Functional Quantum Nodes for Entanglement Distribution over Scalable Quantum Networks, *Science* **316**, 316 (2007).
  - [23] T. Wilk, S. C. Webster, A. Kuhn, and G. Rempe, Single-Atom Single-Photon Quantum Interface, *Science* **317**, 488 (2007).
  - [24] G. Smith and J. Yard, Quantum Communication with Zero-Capacity Channels, *Science* **321**, 1812 (2008).
  - [25] L. Czekaj and P. Horodecki, Purely Quantum Superadditivity of Classical Capacities of Quantum Multiple Access Channels, *Phys. Rev. Lett.* **102**, 110505 (2009).
  - [26] M. Demianowicz and P. Horodecki, Quantum Channel Capacities: Multiparty Communication, *Phys. Rev. A* **74**, 042336 (2006).
  - [27] R. Rom and M. Sidi, Multiple Access Protocols: Performance and Analysis (Springer-Verlag, New York, 1990).
  - [28] V. P. Ipatov, Spread Spectrum and CDMA: Principles and Applications (John Wiley & Sons, Ltd, England, 2005).
  - [29] L. E. Frenzel, Principles of Electronics Communications Systems (McGraw-Hill, New York, 2008).
  - [30] T. M. Cover and J. A. Thomas, Elements of Information Theory (Wiley, New York, 1991), page 407.
  - [31] G. Brassard, F. Bussières, N. Godbout, and S. Lacroix, Multiuser quantum key distribution using wavelength division multiplexing, *Proc. SPIE* **5260**, 149 (2003).
  - [32] P. Townsend, Simultaneous quantum cryptographic key distribution and conventional data transmission over installed fibre using wavelength-division multiplexing, *Electron. Lett.* **33**, 188 (1997).
  - [33] K. Yoshino, M. Fujiwara, A. Tanaka, S. Takahashi, Y. Nambu, A. Tomita, S. Miki, T. Yamashita, Z. Wang, M. Sasaki et al., High-speed Wavelength-division Multiplexing Quantum key Distribution System, *Opt. Lett.* **37**, 223 (2012).
  - [34] G. Brassard, F. Bussières, N. Godbout, and S. Lacroix, Multiuser Quantum Key Distribution Using Wavelength Division Multiplexing, *Proc. SPIE* **5260**, 149 (2003).
  - [35] G. Brassard, F. Bussières, N. Godbout, and S. Lacroix, Entanglement and Wavelength Division Multiplexing for Quantum Cryptography Networks, *AIP Conf. Proc.* **734**, 323 (2004).
  - [36] I. Choi, R. J. Young, and P. D. Townsend, Quantum key distribution on a 10Gb/s WDM-PON, *Opt. Express* **18**, 9600 (2010).
  - [37] J. Roslund, R. Medeiros de Araujo, S. Jiang, C. Fabre, and N. Treps, Wavelength-multiplexed quantum networks with ultrafast frequency combs, *Nat. Photonics* **8**, 109 (2014).
  - [38] S. Yokoyama, R. Ukai, S. C. Armstrong, C. Sornphiphatphong, T. Kaji, S. Suzuki, J. Yoshikawa, H. Yonezawa, N. C. Menicucci, and A. Furusawa, Ultra-large-scale continuous-variable cluster states multiplexed in the time domain, *Nat. Photonics* **7**, 982 (2013).
  - [39] F. Li, L. Z. Zhou, L. Liu, and H. B. Li, A Quantum Search Based Signal Detection for MIMO-OFDM Systems, 18th Int. Conf. Telecommun., 276 (2011).
  - [40] M. Anandan, S. Choudhary, and K. P. Kumar, OFDM for Frequency Coded Quantum Key Distribution, *Int. Conf. Fib. Optics. Photonics.*, 3 (2012).
  - [41] J. Zhang, Y.-X. Liu, S. K. Özdemir, R.-B. Wu, X.-B. Wang, F. F. Gao, X. B. Wang, L. Yan, and F. Nori, Quantum Internet Using Code Division Multiple Access, *Sci. Rep.* **3**, 2211 (2013).
  - [42] J. C. Garcia-Escartin and P. Chamorro-Posada, Quantum Spread Spectrum Multiple Access, *IEEE J. Sel. Top. Quantum. Electron.* **21**, 6400107 (2015).
  - [43] T. S. Humble, Quantum Spread Spectrum Communication, *Quantum Information and Computation IX* **8057**, 80570 (2011).
  - [44] J. C. Garcia-Escartin and P. Chamorro-Posada, Quantum Multiplexing with Optical Coherent States, *Quantum Inf. Comput.* **9**, 573 (2009).
  - [45] M. P. Kennedy, Chaos in The Colpitts Oscillator, *IEEE Transactions on Circuits and Systems* **41**, 771 (1994).
  - [46] Z. G. Shi and L. X. Ran, Microwave Chaotic Colpitts Oscillator: Design, Implementation and applications, *J. of Electromagn. Waves and Appl.* **20**, 1335 (2006).
  - [47] U. Parlitz, L. O. Chua, Lj. Kocarev, K. S. Halle, and A. Shang, Transmission of Digital signals by Chaotic Synchronization, *Int. J. Bif. Chaos* **2**, 973 (1992).
  - [48] L. M. Pecora and T. L. Carroll, Synchronization in Chaotic Systems, *Phys. Rev. Lett.* **64**, 821 (1990).

- [49] K. M. Cuomo and A. V. Oppenheim, Circuit Implementation of Synchronized Chaos with Applications to Communications, *Phys. Rev. Lett.* **71**, 65 (1993).
- [50] J. Zhang, Y.-X. Liu, W.-M. Zhang, L.-A. Wu, R.-B. Wu, and T.-J. Tarn, Deterministic Chaos Can Act as a Decoherence Suppressor, *Phys. Rev. B* **84**, 214304 (2011).
- [51] L. Zhou, S. Yang, Y. X. Liu, C. P. Sun, and F. Nori, Quantum Zeno Switch for Single-photon Coherent Transport, *Phys. Rev. A* **80**, 062109 (2009).
- [52] S. Ashhab, J. R. Johansson, A. M. Zagoskin, and F. Nori, Two-level Systems Driven by Large-amplitude Fields, *Phys. Rev. A* **75**, 063414 (2007).
- [53] J. Bergli, Y. M. Galperin, and B. L. Altshuler, Decoherence in Qubits due to Low-frequency Noise, *New J. Phys.* **11**, 025002 (2009).
- [54] P. van Loock, T. D. Ladd, K. Sanaka, F. Yamaguchi, K. Nemoto, W. J. Munro, and Y. Yamamoto, Hybrid Quantum Repeater Using Bright Coherent Light, *Phys. Rev. Lett.* **96**, 240501 (2006).
- [55] T. D. Ladd, P. van Loock, K. Nemoto, W. J. Munro, and Y. Yamamoto, Hybrid Quantum Repeater Based on Dispersive CQED Interactions Between Matter Qubits and Bright Coherent Light, *New J. Phys.* **8**, 184 (2006).
- [56] A. Blais, R. S. Huang, A. Wallraff, S. M. Girvin, and R. J. Schoelkopf, Cavity Quantum Electrodynamics for Superconducting Electrical Circuits: An Architecture For Quantum Computation, *Phys. Rev. A* **69**, 062320 (2004).
- [57] P. Kolchin, C. Belthangady, S. W. Du, G. Y. Yin, and S. E. Harris, Electro-Optic Modulation of Single Photons, *Phys. Rev. Lett.* **101**, 103601 (2008).
- [58] M. Tsang, Cavity Quantum Electro-Optics, *Phys. Rev. A* **81**, 063837 (2010).
- [59] J. Jing and T. Yu, Non-Markovian Relaxation of a Three-Level System: Quantum Trajectory Approach, *Phys. Rev. Lett.* **105**, 240403 (2010).
- [60] J. Jing, L. A. Wu, M. Byrd, J. Q. You, T. Yu, and Z. M. Wang, Nonperturbative Leakage Elimination Operators and Control of a Three-Level System, *Phys. Rev. Lett.* **114**, 190502 (2015).